Genomic DNA breakpoints in *AML1/RUNX1* and *ETO* cluster with topoisomerase II DNA cleavage and DNase I hypersensitive sites in t(8;21) leukemia

Yanming Zhang*, Pamela Strissel*, Reiner Strick*, Jianjun Chen*, Giuseppina Nucifora†, Michelle M. Le Beau*, Richard A. Larson*, and Janet D. Rowley*‡

*Section of Hematology/Oncology, Department of Medicine, University of Chicago, Chicago, IL 60637; and †Department of Pathology and the Cancer Center, University of Illinois, Chicago, IL 60607

Contributed by Janet D. Rowley, December 27, 2001

The translocation t(8;21)(q22;q22) is one of the most frequent chromosome translocations in acute myeloid leukemia (AML). *AML1/RUNX1* at 21q22 is involved in t(8;21), t(3;21), and t(16;21) in *de novo* and therapy-related AML and myelodysplastic syndrome as well as in t(12;21) in childhood B cell acute lymphoblastic leukemia. Although DNA breakpoints in *AML1* and *ETO* (at 8q22) cluster in a few introns, the mechanisms of DNA recombination resulting in t(8;21) are unknown. The correlation of specific chromatin structural elements, i.e., topoisomerase II (topo II) DNA cleavage sites, DNase I hypersensitive sites, and scaffold-associated regions, which have been implicated in chromosome recombination with genomic DNA breakpoints in *AML1* and *ETO* in t(8;21) is unknown. The breakpoints in *AML1* and *ETO* were clustered in the Kasumi 1 cell line and in 31 leukemia patients with t(8;21); all except one had *de novo* AML. Sequencing of the breakpoint junctions revealed no common DNA motif; however, deletions, duplications, microhomologies, and nontemplate DNA were found. Ten *in vivo* topo II DNA cleavage sites were mapped in *AML1*, including three in intron 5 and seven in intron 7a, and two were in intron 1b of *ETO*. All strong topo II sites colocalized with DNase I hypersensitive sites and thus represent open chromatin regions. These sites correlated with genomic DNA breakpoints in both *AML1* and *ETO*, thus implicating them in the *de novo* 8;21 translocation.

The translocation t(8;21)(q22;q22) is one of the most frequent chromosome translocations in acute myeloid leukemia (AML), primarily in the M2 subtype (1). *AML1* (also called *RUNX1, CBFA2*,) at 21q22 is involved in t(8;21) and other recurrent chromosome translocations, such as t(3;21) and t(16;21) in *de novo* and therapy-related AML (t-AML) and myelodysplastic syndrome as well as in t(12;21), the most common aberration in childhood B cell acute lymphoblastic leukemia (2–8). These translocations result in novel chimeric genes that play an important role in leukemogenesis. In t(8;21), the 5′ part of the *AML1* gene is fused with nearly the entire *ETO* (*MTG8*) gene at 8q22, resulting in an in-frame *AML1–ETO* fusion located on 8q22 (3, 4).

AML1 is a transcription factor and a critical regulator of hematopoietic cell development; it contains the *Runt* DNA binding domain at the N terminus and a transactivation domain at the C terminus (9, 10). The complete 260-kb genomic sequence of *AML1* contains nine exons (11, 12). The genomic breakpoints in *AML1* are located in intron 5 in t(8;21) and t(16;21) and in introns 6–7b in t(3;21). In t(12;21), in contrast, DNA breaks in *AML1* occur within introns 1 or 2 (Fig. 1) (2–7, 11–13). *ETO* contains a region homologous to the *Drosophila* gene *Nervy* and several DNA-binding protein domains (3, 4). Unlike *AML1*, which has multiple partner genes, *ETO* is involved only with *AML1* in t(8;21). *ETO* is about 150 kb in size and contains 13 exons. The breakpoints in *ETO* are located in introns 1b–2 (Fig. 2) (14).

Some specific chromatin structural elements, i.e., topoisomerase II (topo II) DNA cleavage sites, DNase I hypersensitive (HS) sites, and scaffold-associated regions (SARs), at or near the breakpoints of genes have been implicated in chromosome recombination (15–21). Topo II binds preferentially to the scaffold and is essential for chromosome condensation, transcription, and replication (21–24). Many DNase I HS sites are associated with transcriptional regulatory DNA elements at gene boundaries or within genes; some of these sites colocalize with SARs and/or topo II sites (18–30). AT-rich DNA SARs define the attachment sites of chromatin loops in the DNA scaffold-loop model of chromosomes and are presumed to facilitate the entry of transcription, replication, or chromosome condensation protein factors to target sequences (17–22, 26–35).

In previous studies by us and others, these structural elements have been localized in *MLL* and *AF9* (17–20, 36–39). Like *AML1*, *MLL* at 11q23 is also often involved in *de novo* acute leukemia and t-AML/myelodysplastic syndrome. Little is known about the location of these structural elements in *AML1* and *ETO*, or the precise genomic breakpoints in either gene (13, 14, 40); thus the correlation of genomic breakpoints in *AML1* and *ETO* with these structural elements is largely unknown. Our mapping studies of a large series of leukemia patients with *de novo* t(8;21) reveal a strong correlation of genomic breakpoints in *AML1* and *ETO* with *in vivo* topo II DNA cleavage and DNase I HS sites.

Materials and Methods

Cell Lines. We used the BV173 cell line with t(9;22)(q34;q11), the Mono Mac 6 monocytic cell line with t(9;11)(p22;q23), the ML-2 myeloid cell line with t(6;11)(q27;q23), the UoC-M1 myeloid cell line with a complex karyotype, the Kasumi 1 cell line with t(8;21)(q22;q22), and the $CD34^+$ KG-1A cell line (18, 41).

Patients. Thirty-one leukemia patients, including one t-AML patient, were studied with informed consent as described in an Institutional Review Board-approved protocol. Except for three patients aged 3 and 12 years, all patients were between 20 and 79 years old (Table 1). Cytogenetic analysis identified t(8;21)(q22;q22) as the sole chromosome aberration in seven patients, with loss of an X or Y chromosome in 12 patients, and with other or complex chromosome aberrations in 12 patients.

DNA Primers and Probes. Genomic sequences of AF000125 and AF181450 obtained from the GenBank database were aligned with published cDNA sequences for determination of exon and intron boundaries of *AML1* and *ETO*, respectively. Eighty-two and 98 DNA primers of 19–33 bp specific for introns 4–7a of *AML1* and for introns 1b and 1a of *ETO*, respectively, were purchased from

Abbreviations: AML, acute myeloid leukemia; t-AML, therapy-related AML; topo II, topoisomerase II; HS, hypersensitive; DOX, doxorubicin; CML, chronic myelogenous leukemia; BCR, breakpoint cluster region.

‡To whom reprint requests should be addressed at: Section of Hematology/Oncology, Department of Medicine, University of Chicago, 5841 South Maryland Avenue, Chicago, IL 60637. E-mail: jrowley@medicine.bsd.uchicago.edu.

The publication costs of this article were defrayed in part by page charge payment. This article must therefore be hereby marked "*advertisement*" in accordance with 18 U.S.C. §1734 solely to indicate this fact.

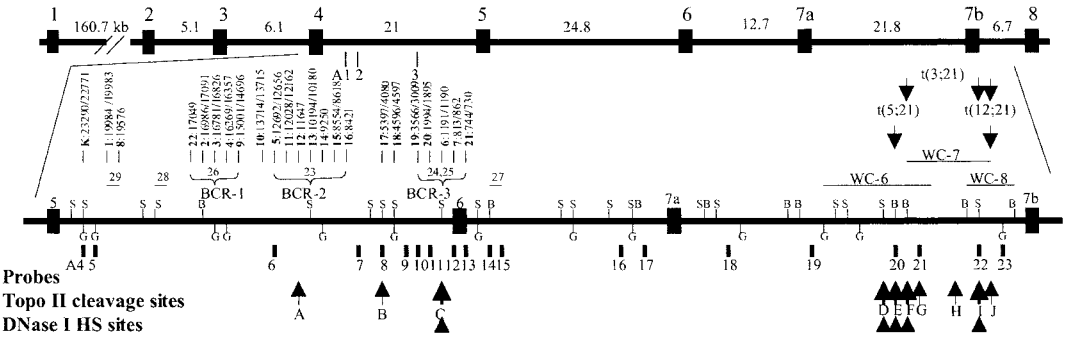

Fig. 1. *In vivo* topo II cleavage, DNase I HS sites, and genomic breakpoints in *AML1* in t(8;21). The vertical boxes and lines represent exons, genomic DNA probes, and *Bam*HI (B), *Bgl*II (G), and *Sac*I (S) restriction sites. Large and small arrows at the bottom represent strong and weak topo II sites, and arrowheads indicate DNase I HS sites. The numbers represent the distance (bp) of the breakpoints to exon 6. Three *AML1* lambda working clones (WC) were integrated in the map. The genomic breakpoints in intron 7a of *AML1* in t(5;21) and t(12;21) (8) as well as in three t-AML with t(3;21) are indicated by arrows. K: Kasumi 1 cell line.

Integrated DNA Technologies, Coralville, IA. Twenty-three and 14 genomic DNA probes of *AML1* and *ETO* were produced with these primers.

***In Vivo* Topo II Cleavage of DNA.** An *in vivo* topo II DNA cleavage assay was carried out according to Strissel *et al.* (18, 20). Cells were treated for 6 h with 5 μM–50 μM etoposide (VP16) (Sigma) or 0.2 μM–1.0 μM doxorubicin (Dox, Sigma). Cell viability measured by trypan blue staining was more than 85%. For cell lines that showed topo II DNA cleavage resistance, the drug concentrations tested were 25 μM–200 μM for VP16 and 1 μM–5 μM Dox for 16 h. For these cell lines, cell viability did not differ from that of controls.

***In Vivo* Topo II Reversibility Analysis.** Topo II-induced DNA cleavage was reversed by two different methods (17, 42, 43). Briefly, the BV173 cells were incubated with 25 μM and 50 μM VP16 for 6 h and 16 h, followed by heat treatment (42) or drug removal (43).

DNase I Treatment of Nuclei. For each hematopoetic cell line, nuclei were isolated and stored according to Mirkovitch *et al.* (28) and our previous studies (18, 20, 44). Nuclei were treated with 2–10 units of DNase I (Sigma) according to Kas and Laemmli (45) and Strissel *et al.* (19).

Southern Blot Analysis. Genomic DNA isolation and restriction digestion was performed as described (17–20). Genomic DNA probes were randomly primed with ^{32}P-dCTP. DNA rearrangements in *AML1* and *ETO* were identified with at least two different DNA restriction digests and different genomic probes.

Long-Distance PCR, Direct Sequencing. Long-distance PCR was performed by using the Taqplus system (Stratagene). PCR products were directly sequenced on an Applied Biosystems Prism 377 sequencer. The BLAST search, MACVECTOR (Oxford Molecular Group, Campbell, CA), and SEQUENCHER (Gene Codes, Ann Arbor, MI) software were used for identifying genomic junctions between *AML1* and *ETO* and for searching for specific recombination-related DNA sequence motifs, including V(D)J recombination sequences, topo II consensus sites, translin binding sequences, *x*-like sequences, and purine/pyrimidine repeat regions.

Results

Cloning Genomic DNA Breakpoints in *AML1* and *ETO* in Leukemia Patients with t(8;21). DNA rearrangements in *AML1* were detected in the Kasumi l cell line and in 29 of the 31 patients. These leukemia patients included 24 adults and three children with *de novo* AML, one adult with t-AML, and one adult with chronic myelogenous leukemia (CML) in an accelerated phase. Genomic breakpoints in *AML1* were identified in intron 5 in 28 patients and intron 6 in the CML patient (Fig. 1). Two DNA rearrangements were detected with probes A4 and A6 on *Bam*HI blots in the Kasumi 1 cell line and patient 5, indicating that the breakpoints in these patients must fall within the region corresponding to the probes. In six patients, including patient 22 with t-AML, genomic breakpoints were located in a 0.8-kb breakpoint cluster region (BCR) (named BCR-1) at the 5′ end of the 18.7-kb *Bam*HI fragment. In eight other patients, breakpoints occurred in a 4.2-kb BCR (BCR-2) in the middle of intron 5. In seven patients, the breakpoints were clustered in a 2.1-kb BCR (BCR-3) 0.6 kb 5′ of exon 6.

In *ETO*, DNA rearrangements were detected in the Kasumi 1 cell line and 27 leukemia patients (Fig. 2). Two DNA rearrange-

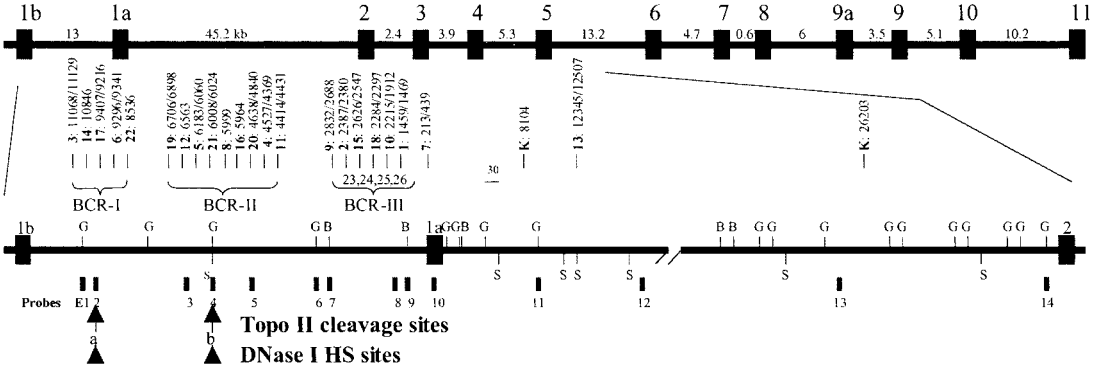

Fig. 2. *In vivo* topo II cleavage, DNase I HS sites and genomic breakpoints in *ETO* in t(8;21). The vertical boxes and lines represent exons, genomic DNA probes, and *Bam*HI (B), *Bgl*II (G) and *Sac*I (S) restriction sites. Arrows and arrowheads at the bottom represent topo II cleavage and DNase I HS sites. The numbers represent the distance (bp) of the breakpoints to exon 1a. K: Kasumi 1 cell line.

Table 1. Leukemia patients with diagnosis, cytogenetic, and sequence results

No.	Age/sex	Diagnosis	Materials	Karyotype and percentage of clones with t(8;21) by cytogenetic analysis: Karyotype	%	Duplications (+)/deletions (−): *AML1* (bp)	*ETO* (bp)
1*	20/M	AML-M2	BM, DX	46,XY,t(4;5)(p14;p15),t(8;21)(q22;q22)[18]/46,idem,−9,+mar[2]	100	No change	No change
2	36/M	AML	BM, RL	46,XY,der(5)t(1;5)(5;?)(q25;p11q31;?),t(8;21)(q22;q22)[19]/44,idem,−4,−11,del(1)(p32p36)[1]	100	+104	−6
3	56/M	AML-M2	BM,DX	46,XY,t(8;21)(q22;q22)[13]/45,idem,−Y[6]/46,XY[4]	83	−44	−60
4*	25/F	AML-M2/M4	BM, DX	45,X,−X,t(8;21)(q22;q22)[8]/46,idem,+15[11]/46,XX[1]	95	+87	+157
5*	27/F	AML-M2	BM, RL	45,X,−X,t(8;21)(q22;q22)[20]/46,XX[2]	91	−35	+122
6	60/M	AML-M2	BM, RL	45,X,−Y,t(8;21)(q22;q22),del(9)(q11or12q31)[28]/46,XY[1]	97	No change	−45
7	3/F	AML-M2	BM, DX	46,XX,t(8;21)(q22;q22)[27]/46,XX[4]	87	−46	−225
8	47/M	AML-M2	BM, DX	46,XY,t(6;21;8)(p23;q22;q22),inv(7)(q31q32orq22q34)x2,inv(9)(p11q13)c[20]	100	Unknown	Unknown
9*	30/F	AML-M2	BM, DX	46,XX,t(8;21)(q22;q22),del(9)(q22q32)[15]/45,idem,−X[7]	100	−305	+143
10	61/F	AML-M2	BM, RL	46,XX,t(8;21)(q22;q22)[12]/46,XX[10]	54	+2	+302
11*	21/M	AML-M2	BM, DX	45,X,−Y,t(8;21)(q22;q22)[21]/46,XY[3]	88	+133	−16
12*	35/F	AML-M2	BM,DX	46,XX,t(8;21)(q22;q22)[3]/47,idem,+4[17]	100	Unknown	Unknown
13*	20/M	AML-M2	BM, DX	46,XY,t(8;21)(q22;q22)[21]/46,idem,del(9)(q13q31)[2]	100	−13	+161
14	43/F	AML-M2	BM, DX	46,XX,t(8;21)(q22;q22)[19]/46,XX[1]	95	Unknown	Unknown
15	75/M	AML-M2	PB, DX	45,X,−Y,t(8;21)(q22;q22)[24]/46,XY[1]	96	+63	+51
16*	32/M	AML-M2	PB, DX	46,XY,t(8;21)(q22;q22)[21] (in BM)	100	Unknown	Unknown
17*	49/M	AML-M2	PB, DX	45,X,−Y,t(8;21)(q22;q22)[31]	100	−1316	+190
18	27/F	AML-M2	BM, DX	46,XX,t(8;21)(q22;q22)[21]	100	+1	−12
19	12/F	AML-M2	BM, DX	46,XX,t(8;21)(q22;q22)[19]/46,idem,del(9)(q22q31)[3]	100	−556	−191
20*	12/M	AML-M2	BM, DX	46,XY,t(8;21)(q22;q22),del(9)(q13q22)[29]/46,XY[1]	97	−98	−201
21	56/F	AML-M2	PB, RL	46,X,−X,der(2)t(2;8)(q31;q11),t(8;21)(q22;q22)[5]/45,idem,t(8;15)(q13;q15)[4]45,idem,t(12;15)(q22;q13)[3]/45,idem,t(1;1)(p32;q36),t(12;15)[9]/90,XX,−X,−X,t(1;1)x2,+der(2)t(2;8)x2,t(8;21)x2,t(12;15)x2[2] (in BM)	100	−5	−15
22	43/F	HD, t-AML	BM, DX	46,XX,t(8;21)(q22;q22)[20]/46,idem,add(11)(q21or22)[1]/45,idem,−X,add(11)[2]/46,XX[3]	89	Unknown	Unknown
23*	25/F	AML-M2	BM, RL	46,XX,t(8;21)(q22;q22)[8]/46,XX[13]	38	Intron 5	Intron 1b
24	21/M	AML-M2	BM, RL	45,X,−Y,t(8;21)(q22;q22)[1]/45,idem,add(19)(p13.3)[1]/46,XX[18]	10	Intron 5	Intron 1b
25	28/M	AML-M2	PB, DX	45,X,−Y,t(8;21)(q22;q22)[16]/46,XY[9] (in BM)	64	Intron 5	Intron 1b
26*	79/M	AML-M2	BM, DX	46,XY,del(13)(q12q14)[9]/46,idem,t(8;21)(q22;q22)[2]/46,XY,der(8)t(8;21)(q22;q22),del(13),der(21)t(8;21)(q22;q22)t(15;21)(q15;q24)[18]/46,XY[2]	65	Intron 5	Intron 1b
27*	22/M	CML accelerated phase	BM,DX	46,XY,t(9;22)(q34;q11.2)[1]/46,idem,t(8;21)(q22;q22)[18]/47,idem,del(2)(q11.2;q13.3),+8,t(8;21)[5]/48,idem,t(8;21),+der(8)t(8;8)(p11;q21)x2[4]/46,XY[1]	94	Intron 6	Not detected
28	66/M	AML-M2	BM, DX	47,XY,+8,t(8;21)(q22;q22)[14]/48,idem,+12[12]/46,XY[3]	90	Intron 5	Not detected
29*	57/F	AML-M2	BM, DX	45,X,−X,t(8;21)(q22;q22)[30]	100	Intron 5	Not detected
30	58/M	AML-M2	BM	46,XY,t(8;21)(q22;q22)[15]/46,XY[1] (in a sample 1 month earlier)	94	Not detected	Intron 1a
31*	44/M	AML-M2	BM, RL	Complex karyotypes with t(8;21)(q22;q22)†	57	Not detected	Not detected

BM: bone marrow. PB: peripheral blood. DX: diagnosis. RL: relapse. HD: Hodgkin's disease. M: male. F: female. In patients 16, 21, and 25, a t(8;21) was detected by cytogenetic analysis in bone marrow, but only peripheral blood obtained at the same time was available for the study. In patient 30, cytogenetic analysis detected a t(8;21) in a bone marrow sample 1 month earlier than the sample used in this study, which included no cytogenetic information. In patients 8, 12, 16, and 22, *AML1-ETO* fusion junctions only were cloned, whereas in patient 14 *ETO-AML1* fusion only was sequenced. In patient 23–26, genomic fusions between *AML1* and *ETO* have not yet been sequenced.

*Patients included in our previous study (46).

†The karyotype of patient 31 is 92,XXYY,+Y,del(1)(p3?3p3?5),+2,t(2;2)(q35;q37),der(6)t(6;15)(p23;q21.2 or p21;q15),t(7;16)(p1?2;p13),t(8;21)(q22;q22)x2,−11,der(12)t(12;15)(p13;q1?3),−15,−15,add(16)(p13),−17,del(17)(q2?1q2?3),+18,der(19)t(11;19)(q13;q13),t(21;22)(q11;q13)x2,+mar1[9]/94,idem,+mar2,+mar3[4].

ments resulting from splitting of the probes were detected on *Bam*HI, *Hin*dIII, or *Sac*I blots with probe E2 in patients 6 and 17, probe E4 in patients 5 and 19, probe E5 in patient 4, probe E8 in patients 9 and 15, and probe E9 in patient 7. The genomic breakpoints in five patients, including patient 22 with t-AML were clustered in a 1.9-kb BCR (BCR-I) ≈3 kb 3′ of exon 1b. Genomic breakpoints in nine other patients were clustered in a 2.5-kb BCR (BCR-II) in the middle of intron 1b. The third BCR (BCR-III) involving 10 patients was located within a 1.6-kb region 1.6 kb 5′ of exon 1a. Thus, genomic DNA breakpoints were detected in both *AML1* and *ETO* in the Kasumi 1 cell line and 26 leukemia patients. In patients 27 (CML), 28, 29, and 30, DNA rearrangements were detected in *AML1* or *ETO* only. In patient 31, no DNA rearrangement was detected in *AML1* and *ETO* with multiple probes on different DNA digests.

Using long-distance PCR and direct sequencing we cloned genomic junctions between *AML1* and *ETO* in 23 patients. In the Kasumi 1 cell line and 17 patients, both *AML1-ETO* and the reciprocal fusion were sequenced, whereas *AML1-ETO* or *ETO-AML1* only was cloned in five patients (Table 2, which is published as supporting information on the PNAS web site, www.pnas.org). Among these 18 patients, deletions ranging from 5 to 18,098 bp were identified in *AML1* in 10 patients and in *ETO* in 10 patients, whereas duplications of 1 to 302 bp were detected in *AML1* in six

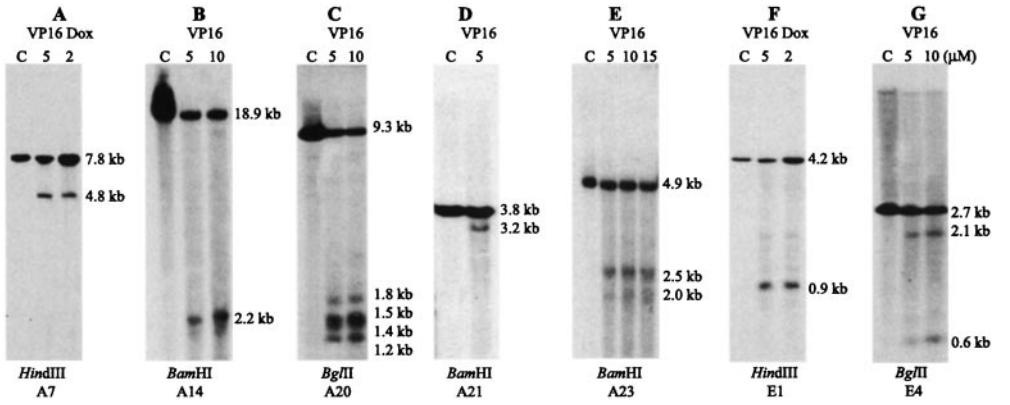

Fig. 3. Topo II DNA cleavage sites in *AML1* (*A–E*) and *ETO* (*F* and *G*). (*A*) *Hin*dIII digestion of the BV173 DNA and hybridization with probe A7. A 4.8-kb DNA fragment was detected (topo II site A). (*B*) *Bam*HI digestion and hybridization with probe A14. A 2.2-kb DNA fragment was detected (topo II site C). (*C*) *Bgl*II digestion and hybridization with probe A20. Four DNA fragments of 1.2 kb, 1.4 kb, 1.5 kb, and 1.8 kb were detected (topo II sites D, E, F, and G clustering in a 0.6-kb region). (*D*) *Bam*HI digestion of the ML-2 DNA and hybridization with A21. A 3.2-kb DNA fragment was detected (topo II site H). (*E*) *Bam*HI digestion and hybridization with probe A23. Two 2.5-kb and 2-kb DNA fragments were detected (topo II sites I and J). (*F*) *Hin*dIII digestion and hybridization with probe E1. A 0.9-kb DNA fragment was detected (topo II site a). (*G*) *Bgl*II digestion and hybridization with probe E4. Two 0.6-kb and 2.1-kb DNA fragments were found, indicating topo II site b and splitting of probe E4. Note topo II sites A, G, H, and J are weaker than other sites. C: control of the BV173 or ML-2 cell line without drug treatment.

patients and in *ETO* in seven patients, respectively (Table 2 and Fig. 5, which is published as supporting information on the PNAS web site). Of 41 DNA fusion junctions involving *AML1* and *ETO* in 23 patients, nine had microhomologies of 1–5 bp and 23 contained nontemplate DNA sequences of 1–18 bp (Table 2). In patient 1, the genomic breakpoint in *AML1* was located within a thymidine repeat region. Genomic breakpoints in *ETO* in patient 14 and in *AML1* in patient 16 occurred in an Alu sequence. In these three patients, the breakpoints in the partner gene were not located in another repeat region. Using the MACVECTOR and SEQUENCHER programs with a minimal match of 70%, we did not identify any specific recombination sequence motifs near the breakpoint junctions. A 14/18 match to *in vitro* topo II consensus sequences was identified at 666 bp 5′ of exon 6, which is located within the BCR-3.

Localizing *in Vivo* Topo II DNA Cleavage Sites and DNase I HS Sites in *AML1* and *ETO*. Because DNA breakpoints in *AML1* in chromosome translocations are clustered in introns 5–7b and in *ETO* in introns 1b–2, we first mapped topo II and DNase I HS sites in these regions, which comprise about 88 kb of *AML1* and 66 kb of *ETO*, using 23 and 14 genomic DNA probes for *AML1* and *ETO*, respectively (Figs. 1 and 2).

Using probe A7, we detected a 4.8-kb *Hin*dIII topo II cleavage fragment in intron 5 of *AML1* (Fig. 3*A*). This site (site A) at 10 kb 5′ of exon 6 is located within BCR-2 and was confirmed with probe A6 as a 7.2-kb *Bam*HI DNA fragment (Fig. 1). Using probe A10 or A11, an extra 4.8-kb *Bam*HI DNA fragment was detected. We assume that this topo II site (site B) is located between BCR-2 and BCR-3 at 5 kb 5′ of exon 6 near the breakpoints in patients 17 and 18 (Fig. 1). Using probe A12, A13, or A14, another topo II cleavage site (site C) was detected about 0.7 kb 5′ of exon 6, which colocalizes with BCR-3 (Figs. 1 and 3*B*). Topo II site C was confirmed with probe A12 or A13 as a 2.1-kb *Hin*dIII DNA fragment. Topo II site C was stronger than sites A and B in Southern blot analysis; topo II sites A and C detected in the BV173 cell line were confirmed in the Mono Mac 6 and UoC-M1 cell lines.

Analysis of 21.8 kb of intron 7a of *AML1* with probe A20 revealed four topo II sites (sites D-G) that clustered in a 0.6-kb region 8.6 kb 5′ of exon 7b (Fig. 3*C*). However, topo II site G was weaker than the others. Using probe A21, a topo II site (site H) was identified about 5.4 kb 5′ of exon 7b (Fig. 3*D*). Using probe A23, topo II sites I and J were detected as 2.5-kb and 2-kb *Bam*HI DNA fragments (Figs. 1 and 3*E*). However, site I is stronger than sites H and J. Using probe A22, topo II site I was confirmed as a 2.4-kb *Bam*HI DNA fragment. No topo II cleavage sites were detected in intron 4 (21 kb), intron 6 (12.7 kb), or intron 7b (6.7 kb). Treatment of the Kasumi 1 and KG-1A cell lines with VP16 and Dox failed to detect any topo II cleavage in *AML1*. Similarly, we did not detect any topo II sites in *MLL* and *AF9* in the KG-1A cell line (18, 20), indicating they are resistant to VP16- or Dox-induced topo II DNA cleavage in these genes.

In *ETO*, extra 0.8-kb *Bgl*II and 0.9-kb *Hin*dIII DNA fragments were detected with probe E1 (Figs. 2 and 3*F*), indicating a topo II site (site a) about 3 kb 3′ of exon 1b. Topo II site a colocalizing with BCR-I was confirmed by probe E2 as 1.9-kb *Bgl*II and 3.3-kb *Hin*dIII DNA fragments. Another topo II site (site b) located within BCR-II was revealed with probes E5 and E6 as a 1.9-kb *Hin*dIII and a 4.3-kb *Bam*HI DNA fragment, respectively. Moreover, topo II site b is covered by probe E4, because hybridization with probe E4 detected two 0.6-kb and 2.1-kb *Bgl*II fragments and two 0.7-kb and 2.2-kb *Hin*dIII DNA fragments (Fig. 3*G*). As in *AML1*, these topo II sites were also detected in the Mono Mac 6 and UoC-M1 cell lines. No topo II cleavage sites were detected in the 3′ portion of intron 1b, intron 1a (45.2 kb), or intron 2 (2.4 kb) of *ETO*.

In *in vivo* topo II DNA cleavage reversibility experiments, topo II sites A-C and H-J in *AML1* and topo II sites a and b in *ETO* were examined. After initial incubation with 25 μM and 50 μM VP16 for 6 h, followed by either heat treatment or drug removal, no DNA breakage was detected (Fig. 6*A*, which is published as supporting information on the PNAS web site); thus, all of these strong and weak topo II sites in both genes were completely reversible. However, these topo II sites were not reversible after treatment with VP16 for 16 h (Fig. 6*B*). These results indicate that, during the drug treatment of the first 6 h, topo II is responsible for DNA cleavage and that DNA religation can occur by means of topo II after heat treatment or drug removal. However, after 16 h treatment, DNA cleavage may then be occurring because of apoptotic DNases.

We also examined the entire 88-kb region in *AML1* and the 66-kb region of *ETO* for DNase I HS sites. Using probes A12 and A15, a DNase I HS site was detected at 0.7 kb 5′ of exon 6 of *AML1*, which colocalizes with topo II site C (Fig. 4*A*). Hybridization with probe 20 revealed three DNase I HS sites colocalizing with topo II sites D, E, and F (Fig. 4*B*). A DNase I HS site located at the same region of topo II site I was detected with probe 22 as a 2.7-kb *Bam*HI fragment (Fig. 4*C*). In *ETO*, two DNase I HS sites that colocalize with topo II sites a and b, respectively, were detected with probe E1 as 1.9-kb and 5.7-kb *Bam*HI DNA fragments (Fig. 4*D*). These two DNase I HS sites were confirmed by probes E2 and E6

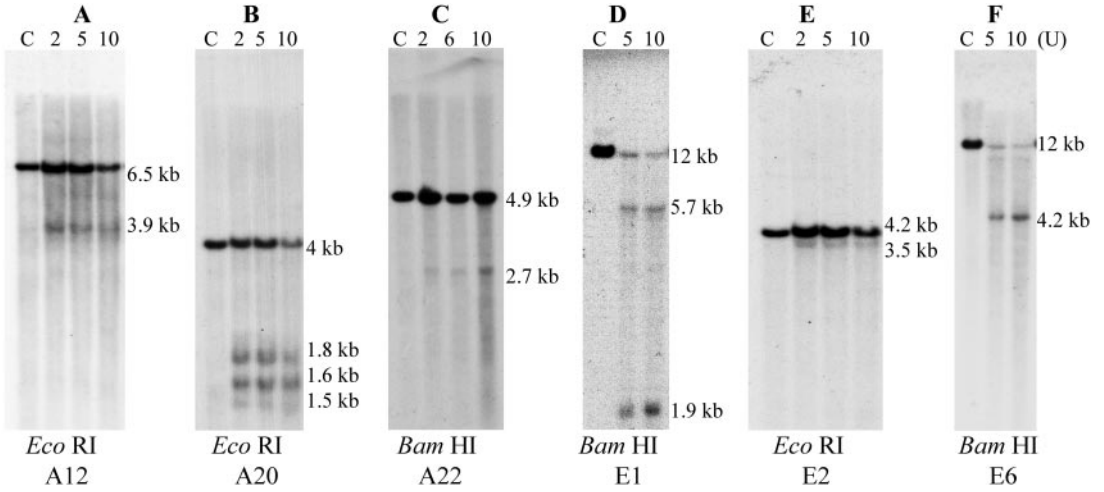

Fig. 4. DNase I HS sites in *AML1* (*A–C*) and *ETO* (*D–F*). (*A*) *Eco*RI digestion and hybridization with A12. A 3.9-kb DNA fragment was detected, indicating a DNase I HS site colocalizing with topo II site C in intron 5. (*B*) *Eco*RI digestion and hybridization with probe A20. Three DNA fragments of 1.5, 1.6, and 1.8 kb were detected, indicating three DNase I HS sites colocalizing with topo II sites D, E, and F. (*C*) *Bam*HI digestion and hybridization with A22. A 2.7-kb DNA fragment was identified, indicating one DNase I HS site colocalizing with topo II site I. (*D*) *Bam*HI digestion and hybridization with probe E1. Two DNA fragments of 1.9 kb and 5.7 kb were detected, thus two DNase I HS sites colocalize with topo II sites a and b, respectively. (*E*) *Eco*RI digestion and hybridization with probe E2. A 3.5-kb DNA fragment was identified, confirming the DNase I HS site that colocalizes with topo II site a. (*F*) *Bam*HI digestion and hybridization with E6. A 4.2-kb DNA fragment was detected, confirming the DNase I HS site colocalizing with topo II site b.

as a 3.5-kb *Eco*RI and a 4.2-kb *Bam*HI fragment, respectively (Fig. 4 *E* and *F*).

Discussion

Clustering of Genomic DNA Breakpoints in *AML1* and *ETO* in the Kasumi 1 Cell Line and Leukemia Patients. Using Southern blot, long-distance PCR and DNA sequencing, we showed that genomic DNA breakpoints in *AML1* in t(8;21) leukemia clustered in three BCRs in intron 5. In our previous study DNA rearrangements in *AML1* were detected in 12 of 15 patients with t(8;21) (46). With multiple digestions and many genomic probes, we defined these breakpoints more accurately in all 12 patients. Moreover, we detected genomic breakpoints in *AML1* in patients 17 and 27, in whom no rearrangement was found in our previous study. In a study of 21 patients with t(8;21), Shimizu *et al.* (13) detected genomic breakpoints in *AML1* in eight and 10 patients in the middle and the 3′ part of intron 5, respectively, which overlap with BCR-1 and BCR-3. Recently, in 16 childhood leukemia patients and two leukemia cell lines with t(8;21), Xiao *et al.* (47) mapped genomic breakpoints in *AML1* in nine patients in the 3′ part of intron 5 that covers BCR-3.

The clustering of genomic breakpoints in *ETO* in t(8;21) is even stronger. The breakpoints in *ETO* in 24 patients clustered in three BCRs in intron 1b. Tighe and Calabi (14) identified two BCRs in intron 1b and one BCR in intron 1a in 18 patients. These two BCRs in intron 1b may overlap BCR-I and BCR-II, respectively. In the study by Xiao *et al.* (47), a large BCR was defined spanning the middle and the 3′ portion of intron 1b, thus covering our BCR-II and BCR-III.

Cloning of genomic fusion junctions between *AML1* and *ETO* in the Kasumi 1 cell line and 22 leukemia patients revealed frequent deletions and duplications in *AML1* and *ETO* as well as microhomology and nontemplate DNA at the breakpoint junctions. There were no site-specific or homologous recombination motifs near the junctions. Similar findings were noted in childhood AML with t(8;21) (47); microhomologies were detected in 14 patients and nontemplate DNA in seven patients. In addition, genomic breakpoints in *MLL*, *AF9*, and *AF4* have been cloned in many patients, and similar changes also were observed at breakpoint junctions (1, 38, 48–50). Thus, our results suggest that nonhomologous DNA recombination and repair occurred between *AML1* and *ETO* after DNA double-strand breakage.

Correlation of Topo II Cleavage and DNase I HS Sites with Genomic DNA Breakpoints in *AML1* and *ETO*. In this study, we mapped 10 and two *in vivo* topo II DNA cleavage sites in introns 5 and 7a of *AML1* and in intron 1b of *ETO*, respectively. Based on the genomic sequences of *AML1* and the putative *in vitro* topo II consensus sequence, 22 *in vitro* topo II sites were predicted in the entire *AML1* (12). The *in vivo* topo II site B in intron 5 and topo II site H or I in intron 7a identified in our study may colocalize with some of these predicted *in vitro* topo II sites. These results are similar to our finding in *MLL*; seven topo II cleavage sites were predicted, but only one was confirmed by *in vivo* analysis (17–19). Therefore, topo II appears to recognize DNA structure rather than a DNA-specific sequence (51). Topo II site C is most likely the same site identified earlier by Stanulla *et al.* (40) in a T-acute lymphoblastic leukemia patient and in several lymphoid and myeloid cell lines. Notably, these topo II DNA cleavage sites in *AML1* are correlated with genomic BCRs in leukemia patients. Topo II sites A and C are located within BCR-2 and BCR-3, respectively, whereas topo II site B is within a 0.2-kb region surrounded by the breakpoints of patients 17 and 18 (Fig. 1). In a patient with CML in blast crisis with t(9;22) and t(3;21), the genomic breakpoint in *AML1* was mapped to intron 5, 5 kb 5′ of exon 6, at the same region of topo II site B (52).

Seven topo II DNA cleavage sites are clustered in the 3′ portion of intron 7a of *AML1*. In our ongoing study of t(3;21) patients, genomic breakpoints in *AML1* in three t-AML patients mapped in the regions of topo II sites D-G and I and J (Fig. 1). In our previous fluorescence *in situ* hybridization study, genomic breakpoints in *AML1* in t(5;21) and t(12;21) were located in the same regions (Fig. 1) (8). Thus, genomic breakpoints in *AML1* in t(3;21) and these less common translocations may also be clustered in and thus correlated with topo II cleavage sites.

A stronger correlation of topo II DNA cleavage sites with genomic breakpoints was observed in intron 1b of *ETO* (Fig. 2). Topo II site a is located at the same region as the 1.9-kb BCR-I, whereas topo II site b is within the 2.5-kb BCR-II.

We have also identified five and two DNase I HS sites in *AML1* and *ETO*, respectively, all colocalizing with all strong *in vivo* topo II sites in both genes. Similarly, in *MLL*, *AF9*, and *BCR* involved

in t(9;22) in CML, all DNase I HS sites colocalized only with strong *in vivo* topo II sites (refs. 18–20 and 36–38; unpublished data). These results indicate that topo II preferentially cleaves at specific open chromatin sites that correlate with stronger topo II DNA cleavage sites.

Based on our results and those of others, and by analogy to *MLL* and *AF9*, we propose that our nonhomologous chromosome translocation model, namely, a common mechanism for both *de novo* and t-AML leukemia, is also applicable to the t(8;21) (17,20). No common DNA motifs have been found thus far at DNA breakpoint junctions in *MLL*, *AF9,* and now in *AML1* and *ETO*; moreover, many DNA breakpoints do not colocalize exactly with, but map close to or at a variable distance from the *in vivo* topo II cleavage sites. Stanulla *et al.* (37) identified that the *in vivo* topo II DNA cleavage sites in *MLL* and *AML1* are also targets for apoptotic nucleases. These findings are important for our understanding of a two-step pathway involving both topo II and the apoptotic nucleases (15, 17). We showed that as with *MLL* and *AF9* (17, 20), topo II sites A-C and H-J of *AML1* and a and b of *ETO* were reversible at 6 h but not at 16 h of VP16 treatment (Fig. 6). Thus, for four independent gene loci tested in reversibility experiments, topo II–DNA cleavage complexes formed by drug/topo II/DNA can be repaired and religated. Therefore, DNase I, presumably cellular apoptotic DNases and topo II recognize and cleave at the same DNA sites; however, the timing of topo II- and apoptotic DNase-induced DNA cleavages by VP16 and Dox may be different and only partly overlap. Thus, the first target of VP16 and Dox and other topo II-inhibiting drugs is topo II bound to specific DNA sites, which is reversible; after some time, apoptotic DNases cleave DNA, which is no longer reversible.

We propose that topo II normally functions at these *in vivo* sites to monitor the helicity of DNA during replication, transcription, repair, and condensation. DNA damage and repair at these sites, which could lead to chromosome translocations, is a rare occurrence, but perhaps could be caused by the natural topo II inhibitors such as some bioflavonoids, which we recently proposed as one mechanism for *de novo* infant leukemia involving *MLL* (17). Indeed, we found that the bioflavonoid quercetin induces the same level of *in vivo* topo II DNA cleavage in both *AML1* and *ETO* as the chemotherapy drugs (data not shown). In addition, other DNA-damaging agents such as pesticides and organic chemicals could act at these topo II sites by either inhibiting topo II or cleaving open chromatin (53). Therefore, DNA cleavage is induced at the topo II cleavage sites, followed by complex DNA repair mechanisms including 3′ to 5′ exonucleolytic processing, which may lead to illegitimate recombination between *AML1* and *ETO* in t(8;21). Recently, Eguchi-Ishimae *et al.* (54) reported induction of topo II cleavage sites in *AML1* and *TEL* in immature B cell lines after treatment with VP16 and subsequent detection of *TEL-AML1* fusion. Analysis of the higher-order chromatin structures at BCRs in these genes is necessary to clarify their role in chromosome translocations.

We thank Nancy Zeleznik-Le and Dong-Er Zhang for their helpful comments. This study is supported in part by National Institutes of Health/National Cancer Institute Grants CA40046 and CA42557 (to J.D.R.), CA84405 (to J.D.R., M.M.L., and R.A.L.), and CA67189 and CA72675 (to G.N.), a grant from the G. Harold and Leila Y. Mathers Charitable Foundation (to J.D.R.), and a grant from the Spastic Paralysis Research Foundation of the Illinois-Eastern Iowa Chapter of Kiwanis International (J.D.R.). G.N. is a Scholar of The Leukemia and Lymphoma Society.

1. Rowley, J. D. (1999) *Semin. Hematol.* **36,** 59–72.
2. Nucifora, G. & Rowley, J. D. (1995) *Blood* **86,** 1–14.
3. Miyoshi, H., Shimizu, K., Kozu, T., Maseki, N., Kaneko, Y. & Ohki, M. (1991*) Proc. Natl. Acad. Sci. USA* **88,** 10431–10434.
4. Erickson, P., Gao, J., Chang, K. S., Look, T., Whisenant, E., Raimondi, S., Lasher, R., Trujillo, J., Rowley, J. D. & Drabkin, H. (1992) *Blood* **80,** 1825–1831.
5. Nucifora, G., Birn, D. J., Espinosa, R., III, Erickson, P., Le Beau, M. M., Roulston, D., McKeithan, T. W., Drabkin, H. & Rowley, J. D. (1993) *Blood* **81,** 2728–2734.
6. Gamou, T., Kitamura, E., Hosoda, F., Shimizu, K., Shinohara, K., Hayashi, Y., Nagase, T., Yokoyama, Y. & Ohki, M. (1998) *Blood* **91,** 4028–4037.
7. Golub, T. R., Barker, G. F., Bohlander, S. K., Hiebert, S. W., Ward, D. C., Bray-Ward, P., Morgan, E., Raimondi, S. C., Rowley, J. D. & Gilliland, D. G. (1995) *Proc. Natl. Acad. Sci. USA* **92,** 4917–4921.
8. Roulston, D., Espinosa, R., III, Nucifora, G., Larson, R. A., Le Beau, M. M. & Rowley, J. D. (1998) *Blood* **92,** 2879–2885.
9. Okuda, T., van Deursen, J., Hiebert, S. W., Grosveld, G. & Downing, J. R. (1996) *Cell* **84,** 321–330.
10. Yergeau, D. A., Hetherington, C. J., Wang, Q., Zhang, P., Sharpe, A. H., Binder, M., Marin-Padilla, M., Tenen, D. G., Speck, N. A. & Zhang, D. E. (1997) *Nat. Genet.* **15,** 303–306.
11. Miyoshi, H., Ohira, M., Shimizu, K., Mitani, K., Hirai, H., Imai, T., Yokoyama, K., Soeda, E. & Ohki, M. (1995) *Nucleic Acid Res.* **23,** 2762–2769.
12. Levanon, D., Glusman, G., Bangsow, T., Ben-Asher, E., Male, D. A., Avidan, N., Bangsow, C., Hattori, M., Taylor, T. D. & Taudien, S. (2001) *Gene* **262,** 23–33.
13. Shimizu, K., Miyoshi, H., Kozu, T. & Ohki, M. (1992) *Cancer Res.* **52,** 6945–6948.
14. Tighe, J. E. & Calabi, F. (1995) *Clin. Sci.* **89,** 215–218.
15. Liu, L. F. (1989) *Annu. Rev. Biochem.* **58,** 351–375.
16. Sperry, A. O., Blasquez, V. C. & Garrard, W. T. (1989) *Proc. Natl. Acad. Sci. USA* **86,** 5497–5501.
17. Strick R., Strissel, P. L., Borgers, S., Smith, S. L. & Rowley, J. D. (2000) *Proc. Natl. Acad. Sci. USA* **97,** 4790–4795.
18. Strissel, P. L., Gill-Super, H., Thirman, M. J., Pomykala, H., Yonebayashi, Y., Tanabe, S., Zeleznik-Le, N. & Rowley, J. D. (1996) *Blood* **87,** 1912–1922.
19. Strissel, P. L., Strick, R., Rowley, J. D. & Zeleznik-Le, N. (1998) *Blood* **92,** 3793–3803.
20. Strissel, P. L., Strick, R., Tomek, R. J., Roe, B. A., Rowley, J. D. & Zeleznik-Le, N. (2000) *Hum. Mol. Genet.* **9,** 1671–1679.
21. Laemmli, U. K., Kas, E., Poljak, L. & Adachi, Y. (1992) *Curr. Opin. Genet. Dev.* **2,** 275–285.
22. Strick, R. & Laemmli, U. K. (1995) *Cell* **83,** 1137–1148.
23. Adachi, Y., Luke, M. & Laemmli, U. K. (1991) *Cell* **64,** 137–148.
24. Watt, P. M. & Hickson, I. D. (1994) *Biochem. J.* **303,** 681–695.
25. Bouilikas, T. (1995) *Int. Rev. Cytol.* **162,** 279–388.
26. Phi-Van, L. & Stratling, W. H. (1988) *EMBO J.* **3,** 655–664.
27. Razin, S. V., Shen, K., Ioudinkova, E. & Scherrer, K. (1999) *J. Cell. Biochem.* **74,** 38–49.
28. Mirkovitch, J., Mirault, M. & Laemmli, U. K. (1984) *Cell* **39,** 223–232.
29. Bode, J. & Maass, K. (1988) *Biochemistry* **27,** 4706–4711.
30. Cockerill, P. N. & Garrard, W. T. (1986) *Cell* **44,** 273–282.
31. Strissel, P. L., Dann, H. A., Pomykala, H. M., Diaz, M. O., Rowley, J. D. & Olopade, O. I. (1998) *Genomics* **47,** 217–229.
32. de Lange, T. (1992) *EMBO J.* **11,** 717–724.
33. Betz, A. G., Milstein, C., Gonzalez-Fernandez, A., Pannell, R., Larson, T. & Neuberger, M. S. (1994) *Cell* **77,** 239–248.
34. Forrester, W. C., van Genderen, C., Jenuwein, T. & Grosschedl, R. (1994) *Science* **265,** 1221–1225.
35. Jenuwein, T., Forrester, W. C., Fernandez-Herrero, L. A., Laible, G., Dull, M. & Grosschedl, R. (1997) *Nature (London)* **385,** 269–272.
36. Aplan, P. D., Chervinsky, D. S., Stanulla, M. & Burhans, W. C. (1996) *Blood* **87,** 2649–2658.
37. Stanulla, M., Wang, J., Chervinsky, D. S., Thandla, S. & Aplan, P. D. (1997) *Mol. Cell. Biol.* **17,** 4070–4079.
38. Domer, P. H., Head, D. R., Renganathan, N., Raimondi, S. C., Yang, E. & Atlas, M. (1995) *Leukemia* **9,** 1305–1312.
39. Zhou, R. H., Wang, P., Zou, Y., Jackson-Cook, C. K. & Povirk, L. F. (1997) *Cancer Res.* **57,** 4699–4702.
40. Stanulla, M., Wang, J., Chervinsky, D. S. & Aplan, P. D. (1997) *Leukemia* **11,** 490–498.
41. Allen, R. J., Smith, S. D., Moldwin, R. L., Lu, M. M., Giordano, L., Vignon, C., Suto, Y., Harden, A., Tomek, R., Veldman, T., *et al.* (1998) *Leukemia* **12,** 1119–1127.
42. Hsiang, Y. H. & Liu, L. F. (1989) *J. Biol. Chem.* **264,** 9713–9715.
43. Borgnetto, M. E., Zunino, F., Tinelli, S., Kas, E. & Capranico, G. (1996) *Cancer Res.* **56,** 1855–1862.
44. Strissel, P. L., Espinosa, R., III, Rowley, J. D. & Swift, H. (1996) *Chromosoma* **105,** 122–133.
45. Kas, E. & Laemmli, U. (1992) *EMBO J.* **11,** 705–716.
46. Nucifora, G., Birn, D. J., Erickson, P., Gao, J., Le Beau, M. M., Drabkin, H. A. & Rowley, J. D. (1993) *Blood* **81,** 883–888.
47. Xiao, Z., Greaves, M. F., Buffler, P., Smith, M. T., Segal, M. R., Dicks, B. M., Wiencke, J. K. & Wiemels, J. L. (2001) *Leukemia* **15,** 1906–1913.
48. Atlas, M., Head, D., Behm, F., Schmidt, E., Zeleznik-Le, N., Roe, B. A., Burian, D. & Domer, P. H. (1998) *Leukemia* **12,** 1895–1902.
49. Reichel, M., Gillert, E., Nilson, I., Siegler, G., Greil, J., Fey, G. H. & Marschalek, R. (1998) *Oncogene* **17,** 3035–3044.
50. Super, H. G., Strissel, P. L., Sobulo, O. M., Burian, D., Reshmi, S. C., Roe, B., Zeleznik-Le, N., Diaz, M. O. & Rowley, J. D. (1997) *Genes Chromosomes Cancer* **20,** 185–195.
51. Udvardy, A. & Schedl, P. (1991) *Mol. Cell. Biol.* **11,** 4973–4984.
52. Hirai, H., Ogawa, S., Kurokawa, M., Yazaki, Y. & Mitani, K. (1999) *Genes Chromosomes Cancer* **26,** 92–96.
53. Alexander, F. E., Patheal, S. L., Biondi. A., Brandalise, S., Cabrera, M. E., Chan, L. C., Chen, Z., Cimino, G., Cordoba, J. C., Gu, L. J., *et al.* (2001) *Cancer Res.* **61,** 2542–2546.
54. Eguchi-Ishimae, M., Eguchi, M., Ishii, E., Miyazaki, S., Ueda, K., Kamada, N. & Mizutani, S. (2001) *Blood* **97,** 737–743.